

Research Article

Xanthone and Flavone Derivatives as Dual Agents with Acetylcholinesterase Inhibition and Antioxidant Activity as Potential Anti-Alzheimer Agents

Inês Cruz,¹ Ploenthip Puthongking,² Sara Cravo,^{1,3} Andreia Palmeira,^{1,3}
Honorina Cidade,^{1,3} Madalena Pinto,^{1,3} and Emília Sousa^{1,3}

¹Laboratório de Química Orgânica e Farmacêutica, Departamento de Ciências Químicas, Faculdade de Farmácia, Universidade do Porto, Rua de Jorge Viterbo Ferreira 228, 4050-313 Porto, Portugal

²Faculty of Pharmaceutical Sciences, Khon Kaen University, Khon Kaen 40002, Thailand

³Centro Interdisciplinar de Investigação Marinha e Ambiental (CIIMAR/CIMAR), Universidade do Porto, Edifício do Terminal de Cruzeiros do Porto de Leixões, Av. General Norton de Matos s/n, 4050-208 Matosinhos, Portugal

Correspondence should be addressed to Honorina Cidade; hcidade@ff.up.pt and Madalena Pinto; madalena@ff.up.pt

Received 14 November 2016; Revised 9 February 2017; Accepted 13 February 2017; Published 26 March 2017

Academic Editor: Sevgi Kolaylı

Copyright © 2017 Inês Cruz et al. This is an open access article distributed under the Creative Commons Attribution License, which permits unrestricted use, distribution, and reproduction in any medium, provided the original work is properly cited.

Alzheimer's disease (AD) is a multifactorial neurodegenerative disorder that is associated with the elderly. The current therapy that is used to treat AD is based mainly on the administration of acetylcholinesterase (AChE) inhibitors. Due to their low efficacy there is a considerable need for other therapeutic strategies. Considering that the malfunctions of different, but interconnected, biochemical complex pathways play an important role in the pathogenesis of this disease, a promising therapy may consist in administration of drugs that act on more than a target on biochemical scenery of AD. In this work, the synthesis and evaluation of xanthone and flavone derivatives as antioxidants with AChE inhibitory activity were accomplished. Among the obtained compounds, Mannich bases **3** and **14** showed capacity to inhibit AChE and antioxidant property, exerting dual activity. Moreover, for the most promising AChE inhibitors, docking studies on the target have been performed aiming to predict the binding mechanism. The results presented here may help to identify new xanthone and flavone derivatives as dual anti-Alzheimer agents with AChE inhibitory and antioxidant activities.

1. Introduction

AD is a neurodegenerative disorder that is characterized by progressive memory loss and cognitive deficits, being the most common form of dementia observed in the elderly [1, 2]. AD is usually designated as a multifactorial disease, because its genesis is associated with a diversity of factors, including genetic, environmental, and endogenous factors. Although the pathogenesis of AD is not yet fully elucidated, the formation of senile plaques, the neurofibrillary tangles, loss of cholinergic neural transmission, and oxidative stress have been identified as the major characteristic hallmarks of this disease [1, 3, 4].

The current therapy for AD is based on the administration of AChE inhibitors, such as tacrine, rivastigmine, donepezil,

and galantamine [1]. However, this therapeutic strategy only is capable of treating the symptoms of AD resulting in favoring of behavioral and cognitive improvements on AD patients [2]. Concerning this and that the number of cases of AD is increasing, it is urgent to find new effective therapeutic strategies for the treatment of AD [2, 5].

Currently, one of the most interesting approaches for the treatment of complex diseases, like AD, is based on the "one molecule, multiple targets" paradigm [6, 7]. Among the multipotent approaches, the association of AChE inhibition and antioxidant activity has been considered as an attractive strategy for the treatment of AD [2, 6] and several multipotent natural and synthetic compounds have been developed as potential drug candidates to treat this neurodegenerative disease [2].

Xanthenes and flavones frequently found in nature [8–13] correspond to “privileged structures,” showing a wide variety of biological activities [9, 11, 14–16]. Among these activities, the effect on molecular targets of AD have been widely studied and explored [6, 17–22]. Some xanthenes and flavones have been shown to inhibit AChE and MAO enzymes [20–27], and the aggregation of A β peptides [28–31], as well as to act as antioxidants [21, 32–37].

Herein we describe the synthesis and biological evaluation of xanthone and flavone derivatives with concomitant AChE inhibitory and antioxidant activities. The planning focused on the development of aminated derivatives of xanthenes/flavones polyphenols, since FDA-approved acetylcholinesterase inhibitors for AD consist of amine drugs [1]. Moreover, for the most promising AChE inhibitors, docking studies on the target have been performed aiming to predict their binding mechanism.

2. Materials and Methods

2.1. Materials. All the reagents and solvents were purchased from Sigma Aldrich and were used without further purification. MW reactions were performed using a glassware setup for atmospheric-pressure reactions and a 100 mL reactor (internal reaction temperature measurements with a fiberoptic probe sensor) and were carried out using an Ethos MicroSYNTH 1600 Microwave Labstation from Milestone. All reactions were monitored by TLC carried out on pre-coated plates (silica gel, 60 F254 Merck) with 0.2 mm of thickness. The purifications of compounds were performed by flash column chromatography using Macherey-Nagel silica gel 60 (0.04–0.063 mm). IR spectra were measured on a KBr microplate in a FTIR spectrometer Nicolet iS10 from Thermo Scientific with Smart OMNI-Transmission Accessory (Software OMNIC 8.3). ^1H and ^{13}C NMR spectra were taken in CDCl_3 (Deutero GmbH) at r.t. or $\text{DMSO}-d_6$ (Deutero GmbH) at r.t., on Bruker Avance 300 instruments (300.13 MHz for ^1H and 75.47 MHz for ^{13}C). ESI-HRMS experiments were performed at CACTI, University of Vigo (Spain), on an APEXQe FT-ICR MS (Bruker Daltonics, USA), equipped with a 7T actively shielded magnet. Ions were generated using a Combi MALDI-electrospray ionization (ESI) source. Ionization was achieved by electrospray, using a voltage of 4500 V applied to the needle and a counter voltage of 300 V applied to the capillary. Samples were prepared by adding a spray solution of 70:29.9:0.1 (v/v/v) $\text{CH}_3\text{OH}/\text{water}/\text{formic acid}$ or 70:29.9:0.1 (v/v/v) $\text{CH}_3\text{CN}/\text{water}/\text{formic acid}$ to a solution of the sample at a v/v ratio of 1 to 5% to give the best signal-to-noise ratio. Data acquisition was performed using the ApexControl software version 3.0.0, and data processing was performed using the DataAnalysis software, version 4.0, both from Bruker Daltonics. Melting points were obtained in a Köfler microscope and are uncorrected. The purity of each compound was determined by analytical HPLC-DAD performed on a SpectraSYSTEM (Thermo Fisher Scientific, Inc., USA) equipped with a P4000 pump, an AS3000 autosampler, and a diode array detector UV8000. The separation was carried out on a 250 \times 4.6 mm i.d. FortisBIO C18 (5 μm) (Fortis™ Technologies

Ltd., Cheshire, UK). ChromQuest 5.0 (version 3.2.1) software (Thermo Fisher Scientific Inc.) managed chromatographic data. Methanol (HPLC grade) was obtained from Carlo Erba Reagents (Val de Reuil, Italy), acetic acid (HPLC grade) was obtained from Romil Pure Chemistry (Cambridge, UK), and HPLC grade water was obtained from Simplicity® UV Ultrapure Water System, Millipore Corporation (USA). Prior to use, mobile phase solvents were degassed in an ultrasonic bath for 15 min. All synthesized compounds possessed a purity of at least 95%.

3,6-Dihydroxy-9-oxo-9H-xanthene-9-one (**4**) and 4-hydroxy-3-methoxy-9-oxo-9H-xanthene-1-carbaldehyde (**10**) were obtained according to described procedures [38, 39].

2.2. Chemistry

2.2.1. 1,3,8-Trihydroxy-9H-xanthene-9-one (**1**)

Method A (Eaton's Reaction). A mixture of phosphorus pentoxide (1.00 g, 3.50 mmol) and methanesulfonic acid (15 mL) was heated on a steam bath (90 °C) until a clear solution was obtained (30 min). Then, a mixture of phloroglucinol (0.38 g, 3 mmol) and 2,6-dihydroxybenzoic acid (0.46 g, 3 mmol) was added to the reaction mixture. This mixture was stirred at reflux (80 °C) for 1 h and the progress of the reaction was monitored by TLC. Then, the resulting mixture was slowly poured into crushed ice and allowed to stand overnight in the fridge. The solid was collected by filtration, washed with water, and dried in oven (60 °C). The crude product was purified by flash column chromatography (SiO_2 , petroleum ether: EtOAc (9 : 1 v/v)) to afford **1** (yield: 2.07%).

Method B (GSS Reaction). A mixture of zinc chloride (13.25 g, 97.2 mmol) and phosphorus oxychloride (55 mL) was submitted to microwave irradiation at 400 W of potency during 10 min at 60 °C. Then, the 2,6-dihydroxybenzoic acid (5.00 g, 32.40 mmol) was added and the reaction mixture was subjected to microwave irradiation at 400 W of power for 10 min at 60 °C. Finally, phloroglucinol (4.10 g, 32.40 mmol) was added and the mixture was submitted to microwave irradiation at 400 W of power during 60 min at 60 °C. After cooling, the resulting mixture was poured into crushed ice and extracted successively with CH_2Cl_2 (9 \times 200 mL) and a solution of 5% NaHCO_3 (3 \times 250 mL). The organic layers were joined and dried over anhydrous Na_2SO_4 and evaporated under reduced pressure. The crude product was purified by flash column chromatography (SiO_2 , *n*-hexane: EtOAc (9.5 : 0.5 v/v)) to give compound **1** as yellow solid (yield: 2.38%). mp 219–220 °C; IR (KBr, ν (cm^{-1})): 3500–3400 (OH); 1663 (C=O); 1601, 1565, 1514, 1483 (aromatic C=C); 1293 (C-O); ^1H NMR (300 MHz, $\text{DMSO}-d_6$), δ (ppm): 11.89 (1 H, s, OH-1), 11.81 (1 H, s, OH-8), 7.68 (1 H, brt, $J = 8.4$ Hz, H-6), 7.00 (1 H, dd, $J = 8.4, 0.9$ Hz, H-5), 6.79 (1 H, dd, $J = 8.4, 0.9$ Hz, H-7), 6.38 (1 H, d, $J = 2.1$ Hz, H-4), 6.21 (1 H, d, $J = 2.1$ Hz, H-2); ^{13}C NMR (75.47 MHz, $\text{DMSO}-d_6$), δ (ppm): 183.26 (C-9), 167.06 (C-3), 162.16 (C-1), 160.27 (C-8), 157.51 (C-4a), 155.49 (C-10a), 137.18 (C-6), 110.60 (C-7), 107.10 (C-5), 106.88 (C-8a), 101.00 (C-9a), 98.70 (C-2), 94.48 (C-4).

2.2.2. 1,8-Dihydroxy-3-methoxy-9H-xanthen-9-one (2). A mixture of 1,3,8-trihydroxyxanthone (1) (0.30 g, 1.23 mmol), methyl iodide (0.803 mL, 12.30 mmol), and anhydrous K_2CO_3 (0.21 g, 1.24 mmol) in anhydrous acetone (40 mL) was stirred at reflux (60°C) for 3 h. Then, the solid was filtered, the solvent was removed under reduced pressure, and the crude product was purified by crystallization with acetone and by flash column chromatography (SiO_2 , *n*-hexane) to yield compound **2** as yellow needle solid (yield: 74%). mp 170–172°C; IR (KBr, ν (cm^{-1})): 3500–3400 (OH); 1662 (C=O); 1603, 1568, 1505, 1470 (aromatic C=C); 2959, 2925, 2852 (aliphatic C-H); 1294 (C-O); 1H NMR (300 MHz, $CDCl_3$), δ (ppm): 11.99 (1 H, s, OH-1), 11.92 (1 H, s, OH-8), 7.56 (1 H, *brt*, $J = 8.4$ Hz, H-6), 6.87 (1 H, *dd*, $J = 8.4, 0.8$ Hz, H-5), 6.78 (1 H, *dd*, $J = 8.4, 0.8$ Hz, H-7), 6.42 (1 H, *d*, $J = 2.3$ Hz, H-4), 6.35 (1 H, *d*, $J = 2.3$ Hz, H-2), 3.89 (3 H, s, 3-OCH₃); ^{13}C NMR (75.47 MHz, $CDCl_3$), δ (ppm): 184.63 (C-9), 167.35 (C-3), 162.97 (C-1), 161.31 (C-8), 157.78 (C-4a), 156.14 (C-10a), 136.80 (C-6), 110.89 (C-7), 106.96 (C-5), 106.96 (C-8a), 102.70 (C-9a), 97.41 (C-2), 93.10 (C-4), 55.93 (3-OCH₃). ESI-HRMS (+) m/z : Anal. Calcd for $C_{14}H_{11}O_5$ (M+H)⁺: 259.06010; found: 259.06014.

2.2.3. 2-((Dimethylamino)methyl)-1,8-dihydroxy-3-methoxy-9H-xanthen-9-one (3). Dimethylamine (0.420 mL, 0.8395 mmol, 4.35 equiv.) was cooled in the ice bath for about 5 min and 37% formaldehyde solution (0.104 mL, 1.28 mmol) and acetic acid (0.965 mL, 16.85 mmol) were added dropwise. The reaction mixture was stirred at room temperature for 1 h and then **2** was added (0.050 g, 0.193 mmol). The mixture was stirred at room temperature for 6 days and then treated with water (5 mL) and stirring was continued for about 12 h. The resulting solid was filtered and the filtrate was treated with 10% NaOH until the pH was 9–10. Finally, the precipitate was also filtered, washed with water, dried, and then purified by flash column chromatography (SiO_2 , petroleum ether : chloroform : ammonium hydroxide (95 : 5 : 1 v/v/v)) to get **3** as yellow solid (yield: 6.29%). mp 118–120°C; IR (KBr, ν (cm^{-1})): 3600–3400 (OH); 1653 (C=O); 1605, 1558, 1539, 1490 (aromatic C=C); 2923, 2853 (aliphatic C-H); 1296 (C-O); 1230 (C-N); 1H NMR (300 MHz, $CDCl_3$), δ (ppm): 12.09 (1 H, s, OH-1), 12.09 (1 H, s, OH-8), 7.55 (1 H, *brt*, $J = 8.3$ Hz, H-6), 6.86 (1 H, *brd*, $J = 8.3$ Hz, H-5), 6.78 (1 H, *brd*, $J = 8.3$ Hz, H-7), 6.44 (1 H, s, H-4), 3.94 (3 H, s, 3-OCH₃), 3.64 (2 H, s, CH₂N), 2.37 (6 H, s, N(CH₃)₂); ^{13}C NMR (75.47 MHz, $CDCl_3$), δ (ppm): 184.33 (C-9), 165.79 (C-3), 161.39 (C-1), 161.39 (C-8), 157.69 (C-4a), 155.96 (C-10a), 136.58 (C-6), 110.90 (C-7), 107.85 (C-5), 106.79 (C-8a), 102.70 (C-9a), 103.5 (C-2), 90.05 (C-4), 56.34 (3-OCH₃), 49.97 (CH₂N), 44.96 (N(CH₃)₂). ESI-HRMS (+) m/z : Anal. Calcd for $C_{21}H_{25}O_6$ (M+H)⁺: 316.11795; found: 316.11740.

2.2.4. 3,6-Dihydroxy-9-oxo-9H-xanthene-4,5-dicarbaldehyde (5). A mixture of 3,6-dihydroxy-9H-xanthen-9-one (**4**, 5.545 g, 0.024 mol) and hexamethylenetetramine (HMTA, 17.1 g, 0.12 mol) was dissolved in AcOH (60 mL). The reaction mixture was refluxed for 3–6 h. After the reaction mixture was cooled down to room temperature, 80 mL of 15% HCl was added to the reaction. The mixture was refluxed

again for 30 min and cooled down to room temperature. Then, crushed ice was added to the reaction mixture and stirred for 15 min. The solution was kept in refrigerator for overnight. The solid thus obtained was collected and washed with ice-water to give a brown solid (9.280 g) that was further purified by open column chromatography (SiO_2 , chloroform : acetone, several proportions). The fractions eluted with chloroform : acetone (9 : 1) were gathered and the solvent evaporated to furnish a white solid corresponding to 3,6-dihydroxy-9-oxo-9H-xanthene-4,5-dicarbaldehyde (**5**, yield: 4.0%). mp >220°C; 1H NMR (300 MHz, DMSO- d_6), δ (ppm): 10.65 (2 H, s, 4-CHO, 5-CHO), 8.25 (2 H, *d*, $J = 8.8$ Hz, H-1, H-8), 7.07 (2 H, *d*, $J = 8.8$ Hz, H-2, H-7); ^{13}C NMR (75.47 MHz, DMSO- d_6), δ (ppm): 191.12 (4-CHO, 5-CHO), 172.69 (C-9), 166.67 (C-3, C-6), 156.76 (C-10a, C-4a), 133.89 (C-1, C-8), 115.28 (C-2, C-7), 113.89 (C-8a, C-9a), 109.86 (C-4, C-5). ESI-HRMS (+) m/z : Anal. Calcd for $C_{15}H_9O_6$ (M+H)⁺: 285.03936; found: 285.03902.

2.2.5. General Procedure for the Reductive Amination. The carbaldehyde xanthone (**5** or **10**, 0.1 mmol) was dissolved in methanol (5 mL) and 2.4 equivolar of the appropriate amine (0.24 mmol) was added to the solution under N_2 gas. A 4.0 equivolar quantity of $NaBH(OAc)_3$ (0.4 mmol) was added to the mixture solution. The reaction mixture was stirred at room temperature for 30 min. Then, 2.0 equivolar quantity of AcOH was added to the reaction mixture. The reaction mixture was stirred at room temperature under N_2 gas for overnight. After the solvent was evaporated, the crude product was further purified by flash column chromatography (SiO_2 , chloroform : methanol : ammonium hydroxide (90 : 10 : 2 v/v/v)) to afford compounds **6–9**, **11**, and **12** in 32–51% yield.

(1) 4,5-Bis(((2-(diethylamino)ethyl)amino)methyl)-3,6-dihydroxy-9H-xanthen-9-one (6). Pale yellow solid (yield: 51%). mp >220°C; IR (KBr, ν (cm^{-1})): 3446 (OH, broad spectrum); 1602 (C=O); 1431 (aromatic C=C); 1283 (C-O); 1201 (C-N); 1083 (C-O-C). 1H NMR (300 MHz, DMSO- d_6), δ (ppm): 7.86 (2 H, *d*, $J = 8.8$ Hz, H-1, H-8), 6.73 (2 H, *d*, $J = 8.8$ Hz, H-2, H-7), 4.25 (4 H, s, 4-CH₂, 5-CH₂), 2.85 (4 H, *t*, $J = 6.2$ Hz, CH₂), 2.67 (4 H, *t*, $J = 6.8$ Hz, CH₂), 2.57 (8 H, *m*, CH₂), 0.98 (12 H, *t*, $J = 6.8$ Hz, CH₃); ^{13}C NMR (75.47 MHz, DMSO- d_6), δ (ppm): 173.70 (C-9), 166.70 (C-3, C-6), 155.10 (C-4a, C-10a), 126.40 (C-1, C-8), 117.60 (C-2, C-7), 111.70 (C-8a, C-9a), 107.80 (C-4, C-5), 50.02 (C-CH₂), 46.64 (C-CH₂), 44.80 (C-CH₂), 42.00 (4-CH₂, 5-CH₂), 11.42 (C-CH₃). ESI-HRMS (+) m/z : Anal. Calcd for $C_{27}H_{41}N_4O_4$ (M+H)⁺: 485.31223; found: 485.31119.

(2) 3,6-Dihydroxy-4,5-bis(piperidin-1-ylmethyl)-9H-xanthen-9-one (7). Pale yellow solid (yield: 37%). mp >220°C; IR (KBr, ν (cm^{-1})): 3424 (OH, broad spectrum); 2955 (aliphatic C-H); 1616 (C=O); 1431, 1438 (aromatic C=C); 1289 (C-O); 1200 (C-N); 1087 (C-O-C). 1H NMR (300 MHz, DMSO- d_6), δ (ppm): 7.91 (2 H, *dd*, $J = 8.8, 1.4$ Hz, H-1, H-8), 6.91 (1 H, *d*, $J = 8.7$ Hz, H-2/H-7), 6.78 (1 H, *d*, $J = 8.7$ Hz, H-7/H-2), 4.78 (4 H, s, 4-CH₂, 5-CH₂), 2.61 (8 H, *m*, CH₂N), 1.52 (12 H, *m*, CH₂); ^{13}C NMR (75.47 MHz, DMSO- d_6), δ (ppm): 174.18 (C-9), 164.56 (C-3, C-6), 154.81 (C-4a, C-10a), 126.09 (C-1, C-8), 113.86

(C-2, C-7), 113.03 (C-8a, C-9a), 108.16 (C-4, C-5), 53.41 (C-CH₂N), 48.65 (4-CH₂, 5-CH₂), 30.76 (C-CH₂). ESI-HRMS (+) *m/z*: Anal. Calcd for C₂₅H₃₁N₂O₄ (M+H)⁺: 423.22783; found: 423.22580.

(3) 3,6-Dihydroxy-4,5-bis((4-(2-hydroxyethyl)piperazin-1-yl)methyl)-9H-xanthen-9-one (**8**). Pale yellow solid (yield: 32%). mp >220°C; (KBr, ν (cm⁻¹)): 3454 (OH, broad spectrum); 2925 (aliphatic C-H); 1644 (C=O); 1604, 1525, 1469, 1416 (aromatic C=C); 1323 (C-O); 1221 (C-N); 1075 (C-O-C). ¹H NMR (300 MHz, CDCl₃), δ (ppm): 8.14 (2 H, *d*, *J* = 8.8 Hz, H-1, H-8), 6.83 (2 H, *d*, *J* = 8.8 Hz, H-2, H-7), 4.06 (4 H, *s*, 4-CH₂, 5-CH₂), 3.67 (4 H, *t*, *J* = 5.3 Hz, CH₂OH), 2.25 (20 H, *m*, CH₂); ¹³C NMR (75.47 MHz, CDCl₃), δ (ppm): 170.79 (C-9) 159.30 (C-3, C-6), 149.4 (C-4a, C-10a), 122.64 (C-1, C-8), 109.65 (C-8a, C-9a), 109.37 (C-2, C-7), 101.95 (C-4, C-5), 54.41 (C-CH₂OH), 53.20 (4-CH₂, 5-CH₂), 49.26 (C-CH₂N), 48.15 (C-CH₂N), 47.80 (C-CH₂N).

(4) 1,1'-(((3,6-Dihydroxy-9-oxo-9H-xanthene-4,5-diyl)bis(methylene)bis(piperazine-4,1-diyl)bis(ethan-1-one) (**9**). Pale yellow solid (yield: 42%). mp >220°C; IR (KBr, ν (cm⁻¹)): 3448 (OH, broad spectrum); 2921, 2851 (aliphatic C-H); 1624, 1602 (C=O); 1474, 1430, 1400 (aromatic C=C); 1265 (C-O); 1210 (C-N); 1073 (C-O-C). ¹H NMR (300 MHz, DMSO-d₆), δ (ppm): 7.96 (2 H, *d*, *J* = 8.7 Hz, H-1, H-8), 6.91 (2 H, *d*, *J* = 8.8 Hz, H-2, H-7), 4.05 (4 H, *brs*, 4-CH₂, 5-CH₂), 2.50 (16H, *m*, CH₂), 1.81 (6 H, *s*, CH₃); ¹³C NMR (75.47 MHz, DMSO-d₆), δ (ppm): 168.30 (C-9, COCH₃) 162.80 (C-3, C-6), 155.40 (C-4a, C-10a), 126.40 (C-1, C-8), 113.60 (C-2, C-7), 113.40 (C-8a, C-9a), 109.40 (C-4, C-5), 52.70 (4-CH₂, 5-CH₂), 45.50 (C-CH₂N), 21.20 (C-CH₃). ESI-HRMS (+) *m/z*: Anal. Calcd for C₂₇H₃₃N₄O₆ (M+H)⁺: 509.23946; found: 509.23910.

(5) 1-(((2-(Diethylamino)ethyl)amino)methyl)-4-hydroxy-3-methoxy-9H-xanthen-9-one (**11**). Pale yellow solid (yield: 35%). mp >220°C; IR (KBr, ν (cm⁻¹)): 3448 (OH, broad spectrum); 2921, 2851 (aliphatic C-H); 1624 (C=O); 1607, 1586, 1467 (aromatic C=C); 1320 (C-O); 1203 (C-N); 1071 (C-O-C). ¹H NMR (300 MHz, DMSO-d₆), δ (ppm): 8.00 (1 H, *d*, *J* = 8.5 Hz, H-8), 7.58 (1 H, *d*, *J* = 8.0 Hz, H-6), 7.34 (1 H, *dt*, *J* = 1.7, 8.5 Hz, H-7), 7.05 (1 H, *s*, H-2), 6.73 (1 H, *d*, *J* = 8.8 Hz, H-5), 4.20 (2 H, *s*, 1-CH₂), 3.86 (3 H, *s*, 3-OCH₃), 2.71 (2 H, *t*, *J* = 6.09 Hz, CH₂), 2.50 (6 H, *m*, CH₂), 0.94 (6 H, *t*, *J* = 7.1 Hz, CH₃); ¹³C NMR (75.47 MHz, DMSO-d₆), δ (ppm): 177.26 (C-9), 161.11 (C-8b), 154.60 (C-3), 151.50 (C-10a), 147.16 (C-4), 134.82 (C-6), 125.83 (C-8), 123.71 (C-7), 121.67 (C-1), 121.28 (C-8a), 117.58 (C-9a), 113.55 (C-5), 110.92 (C-2), 55.82 (C-CH₂), 52.14 (C-CH₂), 51.75 (1-CH₂), 46.20 (3-OCH₃), 45.51 (C-CH₂), 11.70 (C-CH₃). ESI-HRMS (+) *m/z*: Anal. Calcd for C₂₁H₂₇N₂O₄ (M+H)⁺: 371.19653; found: 371.19573.

(6) 4-Hydroxy-1-(((4-(2-hydroxyethyl)piperazin-1-yl)methyl)-3-methoxy-9H-xanthen-9-one (**12**). Pale yellow solid (yield: 39%). mp >220°C; IR (KBr, ν (cm⁻¹)): 3422 (OH, broad spectrum); 2950, 2834 (aliphatic C-H); 1603 (C=O); 1460, 1412 (aromatic C=C); 1274 (C-O); 1235 (C-N); 1079 (C-O-C). ¹H NMR (300 MHz, DMSO-d₆), δ (ppm): 8.10 (1 H, *dd*, *J* = 1.5, 8.0 Hz, H-7), 7.80 (1 H, *dt*, *J* = 1.7, 8.6 Hz, H-8),

7.60 (1 H, *d*, *J* = 7.8 Hz, H-5), 7.41 (1 H, *dt*, *J* = 1.0, 8.0 Hz, H-6), 7.33 (1 H, *s*, H-2), 4.15 (2 H, *s*, 1-CH₂), 3.02 (2 H, *s*, CH₂), 2.93 (2 H, *m*, CH₂), 2.41–2.69 (8 H, *m*, CH₂); ¹³C NMR (75.47 MHz, DMSO-d₆), δ (ppm): 177.14 (C-9), 1172.15 (C-10a), 154.67 (C-3), 151.31 (C-4a), 146.70 (C-4), 134.80 (C-6), 132.74 (C-8), 126.11 (C-1), 123.94 (C-8a), 121.72 (C-7), 117.60 (C-9a), 113.68 (C-5), 108.70 (C-2), 58.33 (C-CH₂OH), 56.03 (3-OCH₃), 52.77 (C-1CH₂), 48.65 (C-CH₂N), 45.65 (C-CH₂N), 43.22 (C-CH₂N). ESI-HRMS (+) *m/z*: Anal. Calcd for C₂₁H₂₅N₂O₅ (M+H)⁺: 385.17580; found: 385.17425.

2.2.6. 8-((Dimethylamino)methyl)-5,6,7-trihydroxy-2-phenyl-4H-chromen-4-one (**14**). To a solution of baicalein (**13**) (0.2 g, 0.74 mmol) in methanol (100 mL) 37% (v/v) formaldehyde solution (0.018 mL, 0.98 mmol) and dimethylamine (1.00 mL, 2.00 mmol) were added dropwise. The mixture was stirred at room temperature for 1 h 30 min. The precipitate was collected, filtered, and washed several times with methanol. Then, the precipitate was purified by flash column chromatography (SiO₂, chloroform : methanol : ammonium hydroxide (90 : 10 : 2 v/v/v)) to afford compound **14** as orange solid (yield: 10.50%). mp 286–288°C; IR (KBr, ν (cm⁻¹)): 3500–3250 (OH); 1667 (C=O); 1608, 1572, 1536, 1468 (aromatic C=C); 2955, 2919 (aliphatic C-H); 1287 (C-O); 1247 (C-N); ¹H NMR (300 MHz, CDCl₃), δ (ppm): 12.52 (1 H, *s*, OH-5), 7.84–7.82 (2 H, *m*, Ar-2',6'-H), 7.54–7.52 (3 H, *m*, Ar-3',4',5'-H), 6.63 (1 H, *s*, H-3), 4.01 (2 H, *s*, CH₂N), 2.45 (6 H, *s*, N(CH₃)₂); ¹³C NMR (75.47 MHz, CDCl₃), δ (ppm): 182.53 (C-4), 162.60 (C-2), 153.65 (C-7), 147.17 (C-8a), 145.43 (C-5), 132.05 (C-4'), 131.43 (C-1'), 129.10 (C-3',5'), 126.02 (C-2',6'), 119.78 (C-6), 105.18 (C-4a), 104.31 (C-3), 98.54 (C-8), 55.39 (CH₂N), 44.47 (N(CH₃)₂).

2.3. Biological Activity

2.3.1. DPPH Radical Scavenging Assay. Scavenging activity for stable 1,1-diphenyl-2-picrylhydrazyl (DPPH) free radical was evaluated according to a method previously described [40–42] with some modifications. A solution of DPPH radical in methanol was prepared daily and protected from light. Reaction mixtures containing 100 μ L of methanol or DMSO solutions of tested compounds (100–1.56 μ M) and 100 μ L of DPPH (0.03 mg/mL) methanolic solution were shaken in a 96-well microtiter plate and incubated for 30 min in darkness at room temperature (until stable absorbance values were obtained). Controls containing 100 μ L of methanol instead of compounds, blanks containing 200 μ L of methanol, and sample's blanks containing 100 μ L of methanol instead of DPPH methanolic solution were also made. The absorbances were measured at 520 nm in a microplate reader (BioTek Instruments, Vermont, US). The percentage of inhibition activity was calculated according to the following formula: DPPH radical scavenging effect (%) = [1 - (Abs_{sample} - Abs_{sample's blank}/Abs_{control} - Abs_{blank})] \times 100. Ascorbic acid was used as positive control. All the tests were performed in triplicate. The scavenging activities of the tested compounds towards DPPH radical were expressed as the effective concentration at which DPPH radical was scavenged by 50% (IC₅₀).

The IC_{50} value was obtained by interpolation from linear regression analysis.

2.3.2. Ferrous Ion Chelating Assay. The chelation of ferrous ions (Fe^{2+}) was assessed by the methodology described by Dinis et al. with modifications [43]. This assay was performed in a 96-well plate and the absorbance was measured at 562 nm. Briefly, 10 μ L of $FeCl_2$ (50 μ M) was added to 50 μ L of methanolic solution of compounds in different concentrations (100–50 μ M) and 120 μ L of methanol. The mixture was allowed to stand 5 min and the reaction was initiated by the addition of 20 μ L of 3-(2-pyridyl)-5,6-bis(4-phenylsulphonic acid)-1,2,4-triazine (ferrozine, 100 μ M) and the mixture was shaken at room temperature for 10 min. Then, the absorbance of the solution was measured in a microplate reader (BioTek Instruments, Vermont, US). Controls containing 50 μ L of solvent instead of compounds and blanks containing 50 μ L of solvent instead of compounds and 20 μ L milliQ™ purified water instead of ferrozine were made. In this assay, sample's blanks containing 20 μ L milliQ purified water instead of ferrozine were also performed. All tests and analyses were carried out in triplicate and EDTA was used as positive control. The percentage of inhibition of Fe^{2+} -ferrozine complex formation was given below: % inhibition = $[(Abs_{control} - Abs_{blank}) - (Abs_{sample} - Abs_{sample's\ blank})] / (Abs_{control} - Abs_{blank}) \times 100$. The chelating activities of the purified compounds towards ferrous ions were expressed as the effective concentration at which Fe^{2+} -ferrozine complex formation was inhibited in 50% (IC_{50}). The IC_{50} value was obtained by interpolation from linear regression analysis.

2.3.3. Copper Chelating Activity. The chelation of copper ions was assessed by the methodology described by Brown et al. [44] and adapted to a 96-well plate [45]. Stock solutions of each compound (1 mM) were prepared in methanol or DMSO. Then 50 μ M of these solutions was prepared with PBS (10 mM) pH 7.4 and 50 μ L of each was taken to 96-well UV plate (well A-D). Afterward, 100 μ L of ultrapure water (well A), or 50 μ L of ultrapure water and 50 μ L $CuSO_4$ (200 μ M) (well B), or 50 μ L of ultrapure water and 50 μ L of $CuSO_4$ (100 μ M) (well C), or 50 μ L of EDTA (500 μ M) and 50 μ L $CuSO_4$ (200 μ M) (well D) were added. The absorption spectra were recorded between 200 and 800 nm in a microplate reader (BioTek Instruments, Vermont, US), and the scans in the presence of 1:1 (green spectrum) and 2:1 (blue spectrum) of copper-to-compound ratios were compared with the scan with compound alone (red spectrum). All tests and analyses were carried out in triplicate.

2.3.4. AChE Inhibitory Assay. AChE inhibitory activity was measured according to the method of Ellman et al. [46] with some modifications using a 96-well plate reader. Briefly, in the performed assay 20 μ L of 0.22 U/mL AChE from *Electrophorus electricus* was added to the wells containing 20 μ L of tested compounds (100 and 75 μ M in methanol or DMSO), 100 μ L of 3 mM 5,5'-dithiobis(2-nitrobenzoic acid) (DTNB), and 20 μ L of 15 mM acetylthiocholine iodide. Absorbance of the colored end product was measured at 412 nm for 10 minutes

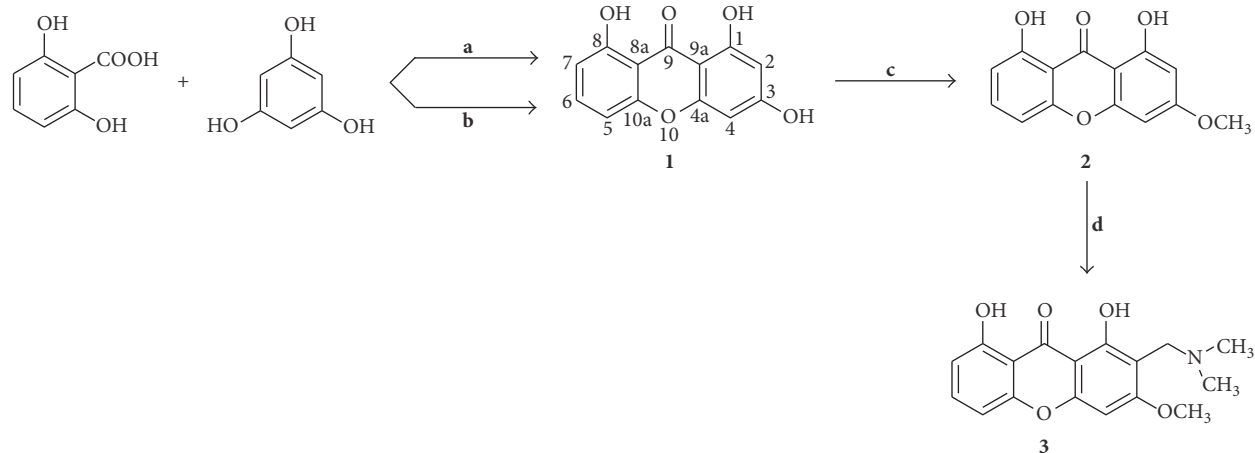
in a microplate reader (BioTek Instruments, Vermont, US). Controls containing 20 μ L of compound vehicle (methanol or DMSO) instead of compounds and blanks containing 20 μ L of buffer (0.1% (w/v) bovine serum albumin in 50 mM Tris-HCl) instead of enzyme and 20 μ L of compound vehicle (methanol or DMSO) instead of compounds were made. In this assay, sample's blanks containing 20 μ L of buffer (0.1% (w/v) bovine serum albumin in 50 mM Tris-HCl) instead of AChE were also performed. Percentage of enzymatic inhibition was calculated as percentage of inhibition = $100 - [(Abs_{sample} - Abs_{sample's\ blank}) / (Abs_{control} - Abs_{blank})] \times 100$. Every experiment was done in triplicate and galantamine was used as positive control. The inhibitory activities of the purified compounds towards AChE were expressed as the effective concentration at which AChE was inhibited by 50% (IC_{50}). The IC_{50} value was obtained by interpolation from linear regression analysis.

2.4. Statistical Analyses. Data were reported as means \pm standard error of the mean (SEM) of at least three independent experiments. Statistical analysis of the results was performed with GraphPad Prism (GraphPad Software, San Diego, CA). Unpaired *t*-test was carried out to test for any significant differences between the means. Differences at the 5% confidence level were considered significant.

2.5. Docking Studies. Crystal structure of AChE (PDB code: 4EY7) [47], downloaded from the protein databank (PDB) [48], was used for the study. Structure files of 14 known AChE inhibitors and compounds 2, 3, 6–9, and 14 were created and minimized using the chemical structure drawing tool Hyperchem 7.5 (Hypercube, FL, USA) [49]. Structure-based docking was carried out using AutoDock Vina (Molecular Graphics Lab, CA, USA) [50]. The active site was defined as the region of AChE that comes within 12 Å from the crystallographic ligand. Default settings for small molecule-protein docking were used throughout the simulations. Top 9 poses were collected for each molecule and the lowest docking score value was associated with the more favorable binding conformation. PyMol1.3 (Schrödinger, NY, USA) [51] and MOE (Chemical Computing Group, Montreal, Canada) [52] were used for visual inspection of results and graphical representations.

3. Results and Discussion

3.1. Chemistry. The synthesis of xanthenes **1**, **2**, and **3** was achieved according to the general reaction pathway outlined in Scheme 1. 1,3,8-Trihydroxyxanthone (**1**) was obtained by one-step synthesis using two different approaches: Eaton's reaction and Grover Shah and Shah (GSS) reaction. In Eaton's reaction, **1** was obtained by the condensation of 2,6-dihydroxybenzoic acid with phloroglucinol in the presence of a mixture of phosphorus pentoxide-methanesulfonic acid (Eaton's reagent) as condensing agent (Scheme 1) [53]. In the GSS reaction xanthone **1** was synthesized by the condensation of the same building blocks in the presence of zinc chloride in phosphorus oxychloride, instead of Eaton's reagent [54] (Scheme 1). Although this condensation agent has been



SCHEME 1: Reagents and conditions for the synthesized xanthenes **1**, **2**, and **3**. (a) Eaton's reaction: P_2O_5/CH_3SO_3H , $90^\circ C$, 30 min; 2,6-dihydroxybenzoic acid/phloroglucinol, $80^\circ C$, 1 h; (b) GSS reaction: (i) $ZnCl_2$, $POCl_3$, MW (400 W), $60^\circ C$, 10 min; (ii) 2,6-dihydroxybenzoic acid, MW (400 W), $60^\circ C$, 10 min; (iii) phloroglucinol, MW (400 W), $60^\circ C$, 60 min; (c) CH_3I , K_2CO_3 , $60^\circ C$, 3 h; (d) Mannich reaction: (i) dimethylamine/ $HCHO/CH_3COOH$, room temperature, 1 h; (ii) addition of xanthone **2**, room temperature, 6 days. The numbering used concerns the NMR assignments.

shown to be efficient for the synthesis of hydroxylated xanthenes, this synthetic methodology is associated with low yields [9, 55, 56]. Taking these into account, some experimental modifications to the classic GSS reaction were performed including the stepwise addition of reactants as described before and the use of microwave assisted organic synthesis (MAOS), instead of conventional thermal heating (classical synthesis). Particularly, in the original GSS methodology, a mixture of a hydroxybenzoic acid, a phenol, fused zinc chloride, and phosphorus oxychloride was heated together on a water bath. Instead, in the GSS reaction here reported, firstly, a mixture of fused zinc chloride and phosphorus oxychloride was irradiated by MW at 400 W for 10 min at $60^\circ C$; then the hydroxybenzoic acid was added and the mixture was subjected to MW irradiation at 400 W for 10 min at $60^\circ C$ and after the irradiation phenol was added and the mixture was once more submitted to MW at 400 W for 60 min at $60^\circ C$ to afford xanthone **1** (Scheme 1). In general, both approaches showed short reaction times (Eaton's reaction: 1 h 30 min; modified GSS reaction by MW: 1 h 20 min) and low yields. Although purification of **1** in both reactions was time consuming, this process was more complex in the GSS reaction. In fact, in this methodology, three different procedures had been performed: extraction with CH_2Cl_2 in order to remove a brown slimy material; extraction with 5% $NaHCO_3$ to eliminate traces of benzoic acid; and a flash column chromatography to get **1**. In contrast, in Eaton's reaction, xanthone **1** was obtained using merely flash chromatography as purification method. In conclusion, according to these results, Eaton's reaction seemed to be more suitable than GSS for the synthesis of **1**, because it was a cleaner approach, requiring less purification procedures.

The hydroxylated xanthone **1** was then methylated with methyl iodide under basic conditions to afford compound **2** (Scheme 1). Following the synthetic route as shown in

Scheme 1, this methylated derivative **2** reacted with formaldehyde and dimethylamine through Mannich reaction to afford the respective Mannich base derivative **3**.

The aminated xanthenes **6–9**, **11**, and **12** were obtained by reductive amination from the corresponding carbaldehydes **5** and **10** (Scheme 2). Both precursors were obtained from oxygenated xanthenes by a Duff formylation according to the described procedures [38, 39].

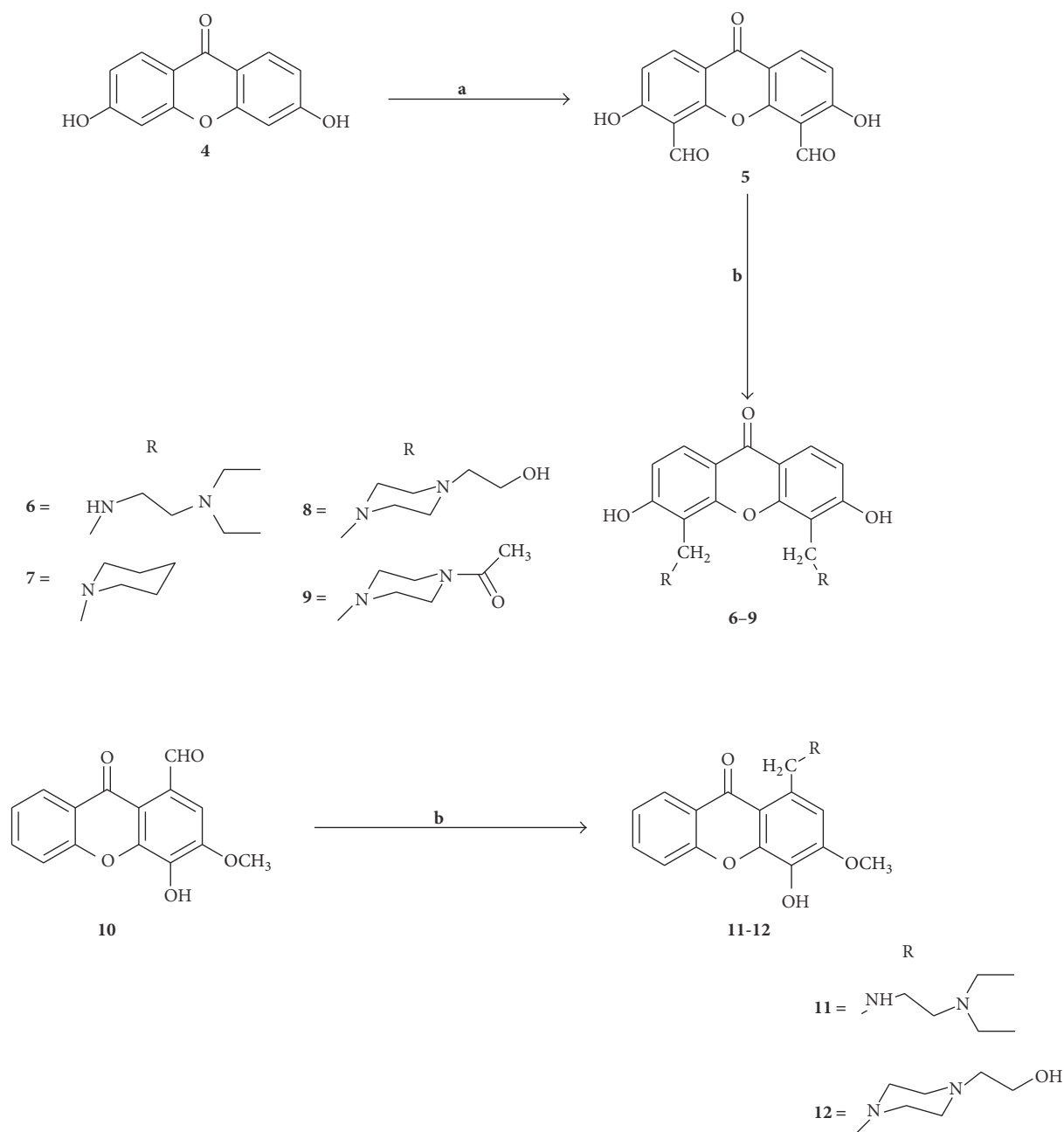
8-((Dimethylamino)methyl)-5,6,7-trihydroxy-2-phenyl-4*H*-chromen-4-one (**14**) was obtained according to the method previously described by Zhang et al. [57]. Concerning this synthetic approach, aminoflavone **14** was achieved from the reaction of baicalein (**13**) with formaldehyde and dimethylamine by Mannich reaction (Scheme 3).

3.2. Biological Activity

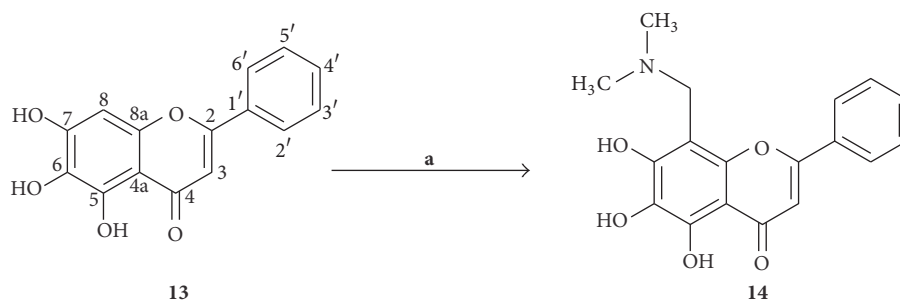
3.2.1. DPPH Radical Scavenging Activity. The DPPH assay has been widely used to assess the antioxidant potential of compounds. Using this assay, the capacity of compounds **1–3**, **6–9**, and **11–14** to transfer labile H-atoms to this free radical was measured (Table 1).

While no promising DPPH radical scavenging activity was observed for xanthenes **1–3** and **6–9** at $100 \mu M$, the aminated derivatives **11** and **12** exhibited some scavenging activity, suggesting that the introduction of amino side chains at C-1, instead of C-4,5, is favorable for this activity. Among the compounds tested the baicalein derivative **14** was the most active, showing an IC_{50} value of $30.40 \pm 1.28 \mu M$, very similar to the precursor baicalein (**13**) ($IC_{50} = 35.09 \pm 4.13 \mu M$), suggesting that the presence of 8-(dimethylamino)methyl group on the flavone skeleton did not significantly alter its ability to scavenge free radicals.

3.2.2. Ferrous Ion Chelating Activity. Among the transition metals, iron is well known as playing a crucial role in



SCHEME 2: Reagents and conditions for the synthesis of carbaldehyde xanthone **5** and aminated xanthones **6-9** and **11-12**. (a) (1) HMTA/AcOH, reflux, 3 h, (2) 15% HCl, reflux, 30 min; (b) amine (2.4 eq), NaBH(OAc)₃ (4 eq), AcOH (2 eq), MeOH, room temperature, overnight.



SCHEME 3: Reagents and conditions for the synthesized flavone **14**. (a) Dimethylamine/HCHO/MeOH, room temperature, 1 h 30 min. The numbering used concerns the NMR assignments.

TABLE 1: DPPH radical scavenging activity of tested compounds.

Compounds	% of scavenging DPPH radical at 100 μM	IC ₅₀ (μM)
1	n.a.	n.d.
2	n.a.	n.d.
3	n.a.	n.d.
6	5.92 \pm 0.84**	n.d.
7	2.32 \pm 0.25*	n.d.
8	5.74 \pm 0.83*	n.d.
9	n.a.	n.d.
11	69.26 \pm 2.11***	61.62 \pm 0.72***
12	47.09 \pm 1.35***	108.99 \pm 0.87***
13	96.03 \pm 0.42***	35.09 \pm 4.13***
14	93.93 \pm 0.20***	30.40 \pm 1.28***

Results are given as mean \pm SEM of three independent experiments performed in triplicate; n.a.: not active; n.d.: not determined. Ascorbic acid (positive control): IC₅₀: 20.40 \pm 0.000213 μM *. * p < 0.05; ** p < 0.01; *** p < 0.001.

TABLE 2: Iron chelating activity of tested compounds.

Compounds	% of chelation at 100 μM	IC ₅₀ (μM)
1	12.19 \pm 2.55*	n.d.
2	n.a.	n.d.
3	88.40 \pm 0.56*	65.94 \pm 1.57*
6	n.a.	n.d.
7	n.a.	n.d.
8	n.a.	n.d.
9	n.a.	n.d.
11	n.a.	n.d.
12	n.a.	n.d.
13	18.24 \pm 3.46*	n.d.
14	49.90 \pm 0.23**	100 \pm 0.21**

Results are given as mean \pm SEM of three independent experiments performed in triplicate; n.a.: not active; n.d.: not determined. EDTA (positive control): IC₅₀: 30.66 \pm 0.17 μM **. * p < 0.05; ** p < 0.001.

production of reactive oxygen species (ROS) by Fenton reaction, which contribute to the oxidative stress commonly found in AD [58]. The ability of compounds **1–3**, **6–9**, and **11–14** to chelate ferrous ions (Fe²⁺) was evaluated by the ferrozine-based colorimetric assay. Only compounds **1**, **3**, **13**, and **14** had ferrous ion chelating activity at 100 μM (Table 2).

Among the tested xanthenes, compound **3** was the most potent, showing an IC₅₀ value of 65.94 \pm 1.57 μM . The comparison of the ferrous ion chelating effects of tested xanthenes suggests that not only the presence but also the position of the amino side chains in the xanthone scaffold may influence this effect. In fact, although the presence of amino groups at position C-2 in derivative **3** is associated with a chelating effect, the presence of this group at C-1 (derivatives **11** and **12**) or C-4,5 (derivatives **6–9**) is not associated with any effect. Moreover, when comparing the results obtained for xanthenes **1–3** it is verified that not only the presence of a hydroxyl group instead of a methoxy group at C-3 but

also the presence of a 2-(dimethylamino)methyl group on the xanthonic scaffold can favor the chelating activity.

Considering flavonoids, compounds **13** and **14** showed interesting chelating activity at 100 μM , suggesting that the catechol moiety in the structure of these flavones was associated with their ferrous ion chelating capacity. In fact, it was reported that the presence of *ortho*-OH groups offers appropriate geometric and electronic environments to bind metal ions [6, 21]. Moreover, considering the chelating activity of **13** (% of chelation at 100 μM = 18.24 \pm 3.46) and **14** (% of chelation at 100 μM = 49.90 \pm 0.23), it is possible to infer that the presence of 8-(dimethylamino)methyl group in the baicalein derivative **14** was associated with an improvement of the ferrous ion chelating activity.

3.2.3. Copper Chelating Activity. As iron, copper (II) ions also promote oxidative damage in AD by the generation of ROS via the Fenton reaction. In addition, this transition metal still has the ability to interfere with protein aggregation processes implicated in the pathogenesis of this disease [1, 59, 60]. The copper chelating activity of compounds **1–3**, **6–9**, and **11–14** was assessed by UV-Vis spectroscopy, mainly through the detection of bathochromic shifts in the spectra of the tested compounds in the presence of Cu²⁺ ions at pH 7.4. For this, the UV-Vis spectra of each tested compound in PBS at pH 7.4 alone (red spectra, Figure 1) and in the presence of a solution of 50 μM CuSO₄ (blue spectra, Figure 1) or 25 μM CuSO₄ (green spectra, Figure 1) were recorded. In addition, the UV-Vis spectrum of each compound in the presence of 25 μM CuSO₄ after addition of 25 μM EDTA (pink spectra, Figure 1) was also registered.

The changes observed in the spectrum of xanthone derivative **1** after the addition of Cu²⁺ (blue and green spectra, Figure 1(a)) in comparison with the spectrum in the absence of this metal ion (red spectrum, Figure 1(a)) and the regeneration of the original spectrum (pink spectrum, Figure 1(a)) after the addition of EDTA suggest that **1** has Cu²⁺ chelating effect. Nevertheless, no chelating activity was observed for the **1** methylated derivative (**2**) since all spectra are overlapped (Figure 1(b)).

For xanthone **2** Mannich base derivative (**3**) some chelating activity was observed. In fact, interactions of **3** with Cu²⁺ ions at 25 μM (green spectrum, Figure 1(c)) and 50 μM (blue spectrum, Figure 1(c)) produced bathochromic shift in bands at 250 nm and 370 nm. The comparison of results obtained for **2** and **3** indicates that the aminomethylation at C-2 of xanthone nucleus potentiates its chelating activity. For derivatives **6–9**, **11**, and **12** no chelating activity was detected since the spectrum of each compound in the presence of copper was overlapped with the spectrum of the compound alone (data not shown).

The chelation of Cu²⁺ by baicalein (**13**) and its Mannich base derivative **14** is also evidenced by the changes in the UV-Vis spectra. For baicalein (**13**) a hypochromic shift in band at 266 nm (blue and green spectra, Figure 1(d)) and a slight bathochromic shift in band at 359 nm after the addition of Cu²⁺ were detected. Moreover, the addition of EDTA (pink spectrum, Figure 1(d)) regenerated the original spectrum. For baicalein Mannich base derivative **14** the chelation of this ion

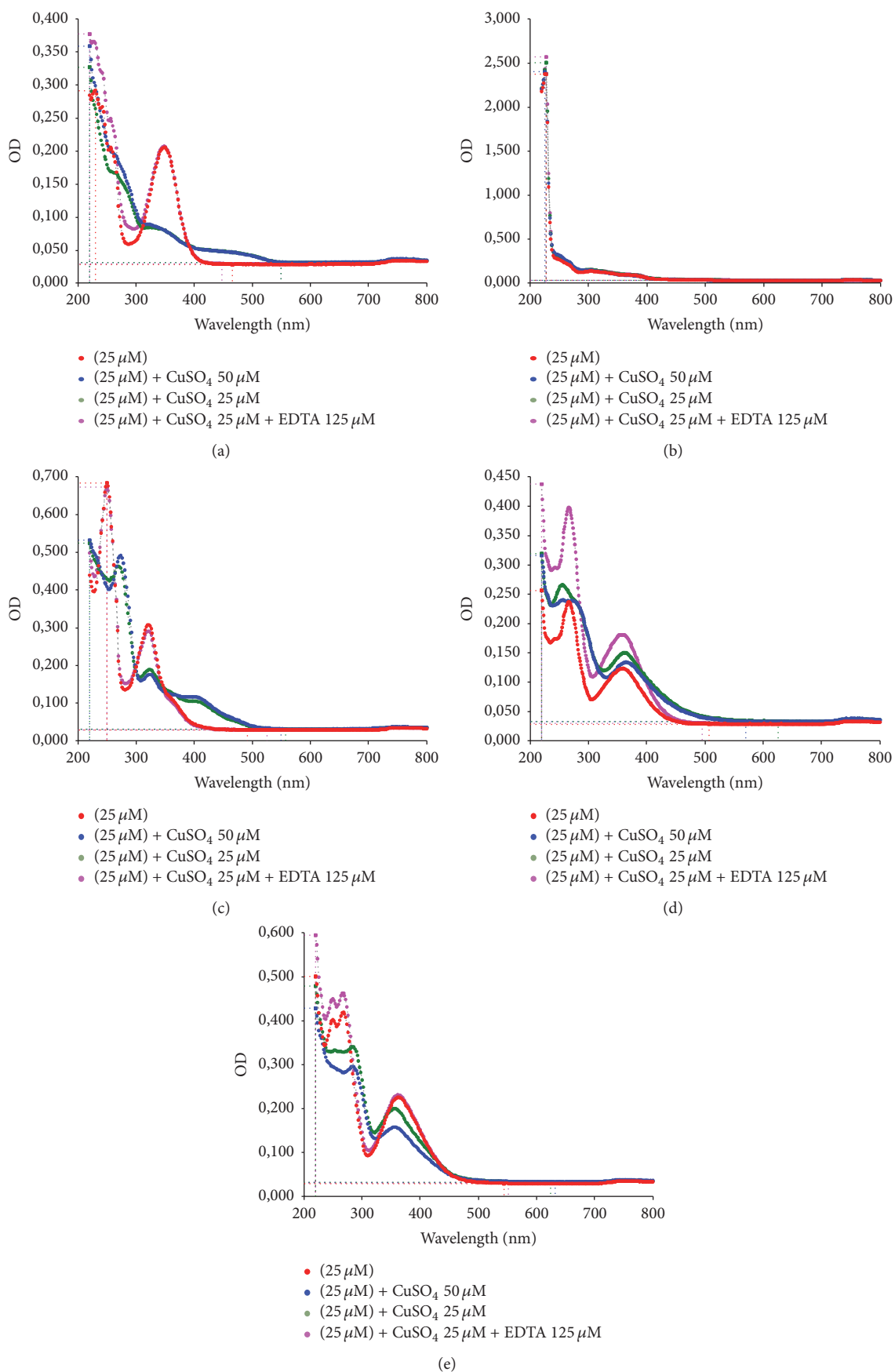


FIGURE 1: UV-Vis spectra of 25 μM of compounds 1 (a), 2 (b), 3 (c), 13 (d), and 14 (e) in PBS at pH 7.4 (red spectra), after the addition of 25 μM CuSO_4 (green spectra), 50 μM CuSO_4 (blue spectra), and 25 μM of CuSO_4 plus 125 μM of EDTA (pink spectra).

TABLE 3: AChE inhibitory activity of tested compounds.

Compounds	% of inhibition at 100 μM	IC ₅₀ (μM)
1	n.a.	n.d.
2	34.04 \pm 3.12*	n.d.
3	49.08 \pm 2.78**	100.00 \pm 2.76**
6	29.28 \pm 5.79**	n.d.
7	17.34 \pm 2.45*	n.d.
8	21.50 \pm 4.02*	n.d.
9	29.74 \pm 3.70**	n.d.
11	n.a.	n.d.
12	n.a.	n.d.
13	n.a.	n.d.
14	69.34 \pm 0.72**	81.99 \pm 1.16**

Results are given as mean \pm SEM of three independent experiments performed in triplicate; n.a.: not active; n.d.: not determined. Galantamine (positive control): IC₅₀: 6.59 \pm 0.15 μM ** . * $p < 0.05$; ** $p < 0.01$.

induced a bathochromic shift in band at 268 nm for both Cu²⁺ concentrations (50 μM and 25 μM , blue and green spectra, Figure 1(e)) and the original spectrum was recovered after the addition of EDTA (pink spectrum, Figure 1(e)).

3.2.4. AChE Inhibitory Activity. The AChE inhibitory activity of compounds **1–3**, **6–9**, and **11–14** was screened by the Ellman spectrophotometric assay with some modifications (Table 3) [46].

Although no effect was observed for 1,3,8-trihydroxy-xanthone (**1**) and xanthenes **11** and **12** with an amino group at C-1, xanthone derivatives possessing amino groups at C-4,5 (compounds **6–9**) or C-2 (compound **3**) revealed AChE inhibitory activity at 100 μM , being derivative **3** the most potent. Overall, these results indicate that the introduction of an amino side chain at C-2 or 4,5 seems to favor the AChE inhibitory activity relatively to position 1.

Regarding the tested flavones, in opposition to baicalein (**13**) which did not possess AChE inhibitory activity, its derivative **14** was revealed to be a moderate AChE inhibitor, with an IC₅₀ value of 81.99 \pm 1.16 μM . As for xanthone derivatives **1–3**, the introduction of 8-(dimethylamino)methyl group on the flavone skeleton is also associated with the increase of AChE inhibition.

In summary, concerning the results obtained for antioxidant activity (DPPH radical scavenging and ferrous and copper ions chelating activities) and the AChE inhibitory property for all studied xanthenes and flavones, it can be seen that some of them showed both activities. Particularly, Mannich base analogues **3** and **14** exhibited interesting AChE inhibitory effect and antioxidant activity through different ways. While aminoxanthone **3** exerted its antioxidant activity by chelating ferrous and copper ions, aminoflavone **14** was an antioxidant agent through radical scavenging and ferrous and copper ions chelating effects.

3.3. Docking Studies. In this work, compounds **2**, **3**, **6–9**, and **14** have been discovered as AChE inhibitors. Therefore, docking studies were performed for this series along

TABLE 4: Docking scores of known AChE inhibitors and compounds **2**, **3**, **6–9**, and **14**.

Compound	Docking scores (kcal·mol ⁻¹)
Trichlorfon	-5.7
Echothiophate	-5.9
Isoflurophate	-5.9
Pyridostigmine	-6.3
Neostigmine	-7.5
Parathion	-7.6
Rivastigmine	-7.9
Tacrine	-8.8
Ladostigil	-9.1
Physostigmine	-9.1
Huperzine A	-9.7
Ungeremine	-10
Galantamine	-10.2
Donepezil	-12.1
2	-9.1
3	-9.4
6	-7.8
7	-5.7
8	-7.6
9	-7.9
14	-10

with compounds already described in the literature as AChE inhibitors [61], being these used as positive controls. For controls, docking scores values ranging from -5.7 to -12.1 kcal·mol⁻¹ were obtained (Table 4). The most stable complex (**14**: AChE) originated a free binding energy within that range (-10 kcal·mol⁻¹) in accordance with in vitro studies (Table 3). Compounds **2** and **3** are also predicted as forming stable complexes with AChE, with docking scores of -9.1 and -9.4 kcal·mol⁻¹, respectively. Amines **6**, **7**, and **9** presented docking scores of -7.8, -7.6, and -7.9 kcal·mol⁻¹, respectively, whereas less active amine **8** presented a docking score of -5.7 kcal·mol⁻¹ (Table 4).

In order to further understand the binding mode of the most potent inhibitors (**2**, **3**, and **14**) to AChE, a careful inspection of the most stable docking pose of these small molecules was performed (Figure 2). AChE is a serine hydrolase possessing a narrow, long, and hydrophobic cavity composed by two subsites: the esteratic and anionic subsites [61]. The esteratic subsite, where AChE is hydrolyzed to acetate and choline, contains the catalytic triad of three amino acids: Ser203, His447, and Glu334, the lining of which contains mostly aromatic residues that form a narrow entrance to the catalytic Ser203 [62]. The activation of Ser203 allows the acylation between hydroxyl group of that residue and AChE oxygen. In the anionic site, the indole side chain of the conserved residue Trp86 makes a cation- π interaction with the quaternary amino group of AChE. A peripheral site is composed of several aromatic residues, lining a hydrophobic region that traps AChE and transfers it to the deep catalytic site [63].

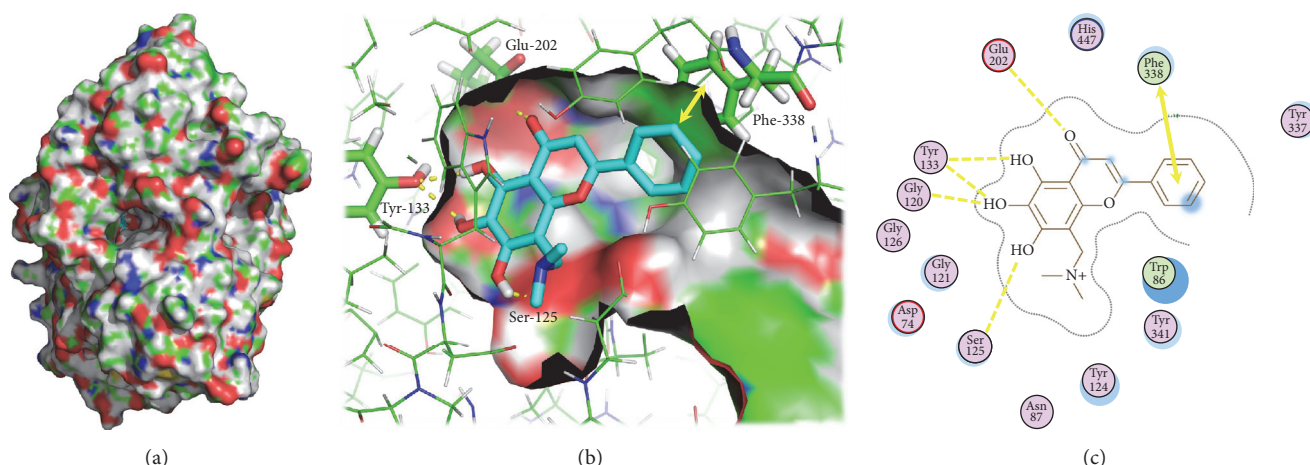


FIGURE 2: (a) AChE (surface) and docked **14** (blue sticks). (b) AChE active site (surface) bound to **14** (blue sticks). Residues involved in hydrogen interactions (yellow broken line) and π stacking interactions (yellow double arrow) are displayed using a stick model. AChE carbon, oxygen, nitrogen, and hydrogen are represented in green, red, blue, and grey, respectively. (c) 2D depiction of the **14** docked into the binding site of AChE highlighting the protein residues that form the main interactions with the different structural units of the inhibitor. Hydrogen-bonding interactions are represented with yellow broken lines. π stacking interactions are represented with a yellow double arrow. Receptor residues that are close to **14**, but whose interactions with the ligand are weak or diffuse, such as collective hydrophobic or electrostatic interactions, are also represented (all the ones that have no indication for hydrogen-bonding or π stacking). Hydrophobic residues are colored with a green interior, polar residues are colored in light purple, basic residues are annotated by a blue ring, and acidic residues are annotated with a red ring. Solvent accessible surface area of **14** is plotted directly onto the atoms in the form of a blue smudge.

The interactions between inhibitors such as donepezil, galantamine, huperzine A, and the enzyme, as observed from their crystallographic structures (Figure 3), are characterized by hydrogen interactions and π - π stacking and cation- π interactions involving aromatic residues of AChE [47]. Most ligands are located at the bottom of the binding groove that forms a hydrophobic pocket base, although larger ligands as donepezil extend to the periphery of the pocket.

The narrower gorge in AChE results in a conformation where the phenyl ring of **14** packs against the aromatic hydrophobic portions of the side chain of Phe338. Packing in this region is quite tight, and only the smallest substituents might be accommodated. In contrast, the chromenone ring system of the flavone molecule faces a larger, negatively charged, and hydrophilic cavity, which includes hydroxyl and carbonyl groups of Gly120, Ser125, Tyr133, and Glu202. Upon analysis of the interaction of **14** in AChE binding site domains, it is observed that the residues Gly120, Ser125, Tyr133, and Glu202 participate in H-interactions. These residues are present in the buried region of the groove. π stacking interactions are established between the phenyl ring of the **14** and Phe338. Although **14** has a protonable amine group, and cation- π interactions between protonated nitrogen and AChE aromatic residues are described as being important for the activity of the highly potent inhibitors, such as donepezil (Figures 3(a) and 3(b)), this interaction is not predicted to occur between **14** and AChE binding site (Figures 2(b) and 2(c)). The binding affinity of **14** allows not only the establishment of several polar interactions, but also stacking interactions with Phe338 favored by the torsion angle between the chromenone and the benzene ring (39.41°). Although 8-(dimethylamino)methyl group of compound **14** is not predicted to be evolved in polar interactions by the

docking algorithm used, it has steric complementarity with a small lateral groove, establishing several van der Waals, hydrophobic, and permanent dipole-induced dipole interactions with residues such as Asp74, Trp86, Asn87, Tyr124, and Ser125.

Compound **3** establishes one polar interaction with residue Tyr124 and one cation- π interaction with Trp86, whereas compound **2** establishes polar interactions with Tyr-337 and His-447 and stacking interactions with Trp86 (Figure 4).

In conclusion, molecular modifications on the flavone scaffold placing the amine group on different positions on A ring will be further explored in order to facilitate a cation- π interaction. Moreover, molecular modifications that would allow the establishment of hydrogen interactions with the catalytic residue Ser203 (described for galantamine; Figures 3(c) and 3(d)) and elongation of the molecule that would favor the establishment of additional π - π or cation- π interactions with residues such as Trp86, Trp286, or Tyr337 (described for donepezil and huperzine A; Figures 3(a), 3(b), 3(e), and 3(f)) are foreseen as being important for the AChE inhibitory ability of flavones.

4. Conclusions

AD is the most prevalent form of dementia and it is known that the malfunctions of different, but interconnected, biochemical complex pathways are related to this pathogenesis. Although inhibition of AChE is one of the most accepted therapy strategies for AD, the AChE inhibitors that have been approved for commercial use show lack of selectivity for AChE and AD patients suffer from side-effects. Therefore,

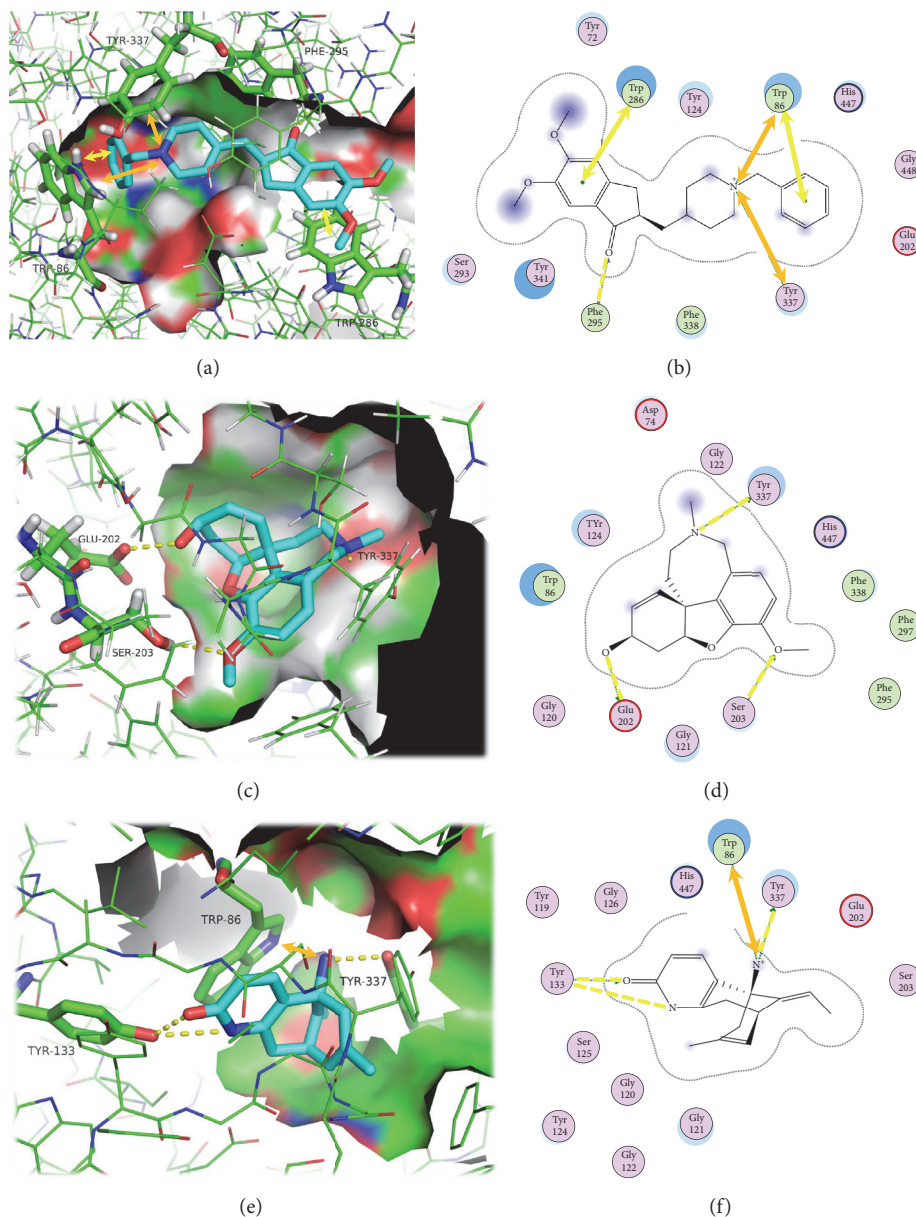


FIGURE 3: AChE active site (surface) bound to crystallographic donepezil (pdb ID: 4EY7) (a), galantamine (pdb ID: 4EY6) (c), and huperzine A (pdb ID: 4EY5) (e) (blue sticks). Residues involved in hydrogen interactions (yellow broken line), π stacking interactions (yellow double arrow), and π -cation interactions (orange double arrow) are displayed using a stick model. AChE carbon, oxygen, nitrogen, and hydrogen are represented in green, red, blue, and grey, respectively. 2D depiction view of crystallographic donepezil (b), galantamine (d), and huperzine A (f) in AChE active site. Hydrogen and π stacking are represented with the same color scheme. Receptor residues that are close to the ligand, but whose interactions with the ligand are weak or diffuse, such as collective hydrophobic or electrostatic interactions, are also represented (all the ones that have no indication for hydrogen-bonding). Solvent accessible surface area of the ligand is plotted directly onto the atoms in the form of a blue smudge. Solvent accessible surface area for the receptor residues is plotted as a blue halo.

this multifactorial disease requires new therapeutic strategies. Considering that concept, the present work focused on obtaining new AChE inhibitors with antioxidant activity based on the xanthonic and flavonic scaffolds. From this study, the Mannich base derivatives **3** and **14** emerged as dual agents with AChE inhibition and antioxidant activity. The synthesis of salt form of these amines to obtain bioactive water-soluble compounds will allow further investigating their potential as dual AChE inhibitors and antioxidants [64].

Conflicts of Interest

The authors declare that there are no conflicts of interest regarding the publication of this paper.

Authors' Contributions

Inês Cruz and Ploenthip Puthongking performed the synthesis, purification, and the evaluation of biological activity

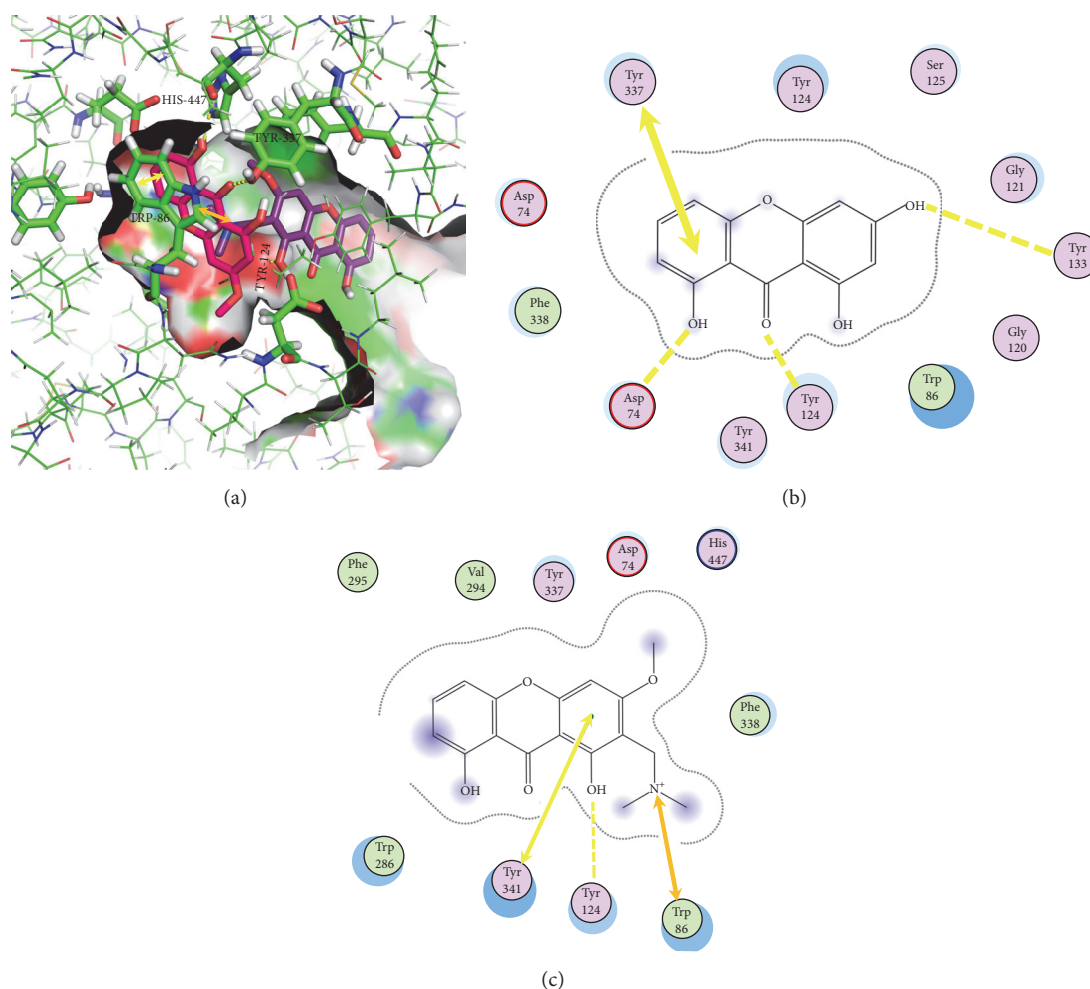


FIGURE 4: AChE active site (surface) bound to **2** (pink sticks) and **3** (purple sticks) (pdb ID: 4EY7) (a); residues involved in hydrogen interactions (yellow broken line), π stacking interactions (yellow double arrow), and π -cation interactions (orange double arrow) are displayed using a stick model. AChE carbon, oxygen, nitrogen, and hydrogen are represented in green, red, blue, and grey, respectively. 2D depiction view of **2** (b) and **3** (c) docked into AChE active site. Hydrogen, π stacking, and π -cation are represented with the same color scheme. Receptor residues that are close to the ligand, but whose interactions with the ligand are weak or diffuse, such as collective hydrophobic or electrostatic interactions, are also represented (all the ones that have no indication for hydrogen-bonding). Solvent accessible surface area of the ligand is plotted directly onto the atoms in the form of a blue smudge. Solvent accessible surface area for the receptor residues is plotted as a blue halo.

(both contributed equally to this work); Sara Cravo contributed to the structure elucidation of compounds; Andreia Palmeira performed the docking studies; Honorina Cidade and Madalena Pinto conceived and designed the work; Honorina Cidade, Madalena Pinto, and Emília Sousa contributed to acquisition, analysis, and interpretation of data and wrote the paper. All authors read, critically revised, and approved the final manuscript.

Acknowledgments

This work was partially supported through national funds provided by FCT/MCTES-Foundation for Science and Technology from the Minister of Science, Technology and Higher Education (PIDDAC) and European Regional Development Fund (ERDF) through the COMPETE-Programa

Operacional Factores de Competitividade (POFC) programme, under the Strategic Funding UID/Multi/04423/2013, the project PTDC/MAR-BIO/4694/2014 (Reference POCI-01-0145-FEDER-016790; Project 3599, Promover a Produção Científica e Desenvolvimento Tecnológico e a Constituição de Redes Temáticas (3599-PPCDT)), PTDC/DTPFTO/1981/2014 (POCI-01-0145-FEDER-016581), and PTDC/AAGTEC/0739/2014 (POCI-01-0145-FEDER-016793) in the framework of the programme PT2020 as well as by the project INNOVMAR-Innovation and Sustainability in the Management and Exploitation of Marine Resources (Reference NORTE-01-0145-FEDER-000035, within Research Line NOVELMAR), supported by North Portugal Regional Operational Programme (NORTE 2020), under the PORTUGAL 2020 Partnership Agreement, through the European Regional Development Fund (ERDF). The authors also thank

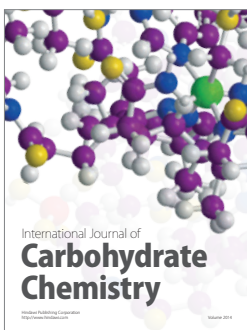
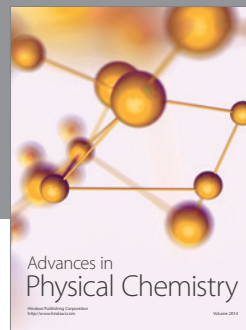
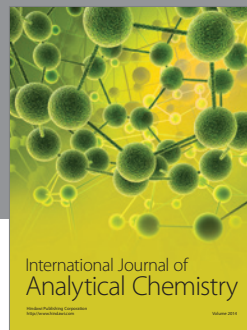
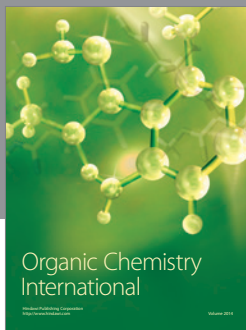
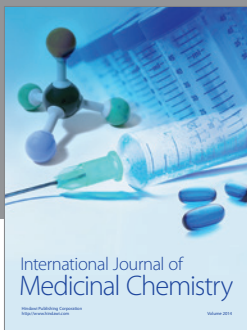
for the grant of Erasmus Mundus Action 2, Lotus Unlimited project of P. Puthongking. This paper is partially based on the Master thesis of Inês Cruz.

References

- [1] A. Cavalli, M. L. Bolognesi, A. Minarini et al., "Multi-target-directed ligands to combat neurodegenerative diseases," *Journal of Medicinal Chemistry*, vol. 51, no. 3, pp. 347–372, 2008.
- [2] N. Guziar, A. Więckowska, D. Panek, and B. Malawska, "Recent development of multifunctional agents as potential drug candidates for the treatment of Alzheimer's disease," *Current Medicinal Chemistry*, vol. 22, no. 3, pp. 373–404, 2015.
- [3] J. D. Grill and J. L. Cummings, "Current therapeutic targets for the treatment of Alzheimer's disease," *Expert Review of Neurotherapeutics*, vol. 10, no. 5, pp. 711–728, 2010.
- [4] K. Fassbender, C. Masters, and K. Beyreuther, "Alzheimer's disease: molecular concepts and therapeutic targets," *Naturwissenschaften*, vol. 88, no. 6, pp. 261–267, 2001.
- [5] S. Kumar, S. A. Khan, L. Bhakuni et al., "Global burden of Alzheimer's disease and promising potential of herbal medicines," *Indian Journal of Drugs*, vol. 1, no. 2, pp. 55–62, 2013.
- [6] H.-Y. Zhang, "One-compound-multiple-targets strategy to combat Alzheimer's disease," *FEBS Letters*, vol. 579, no. 24, pp. 5260–5264, 2005.
- [7] K. S. T. Dias and C. Viegas Jr., "Multi-target directed drugs: a modern approach for design of new drugs for the treatment of Alzheimer's disease," *Current Neuropharmacology*, vol. 12, no. 3, pp. 239–255, 2014.
- [8] J. S. Negi, V. K. Bisht, P. Singh, M. S. M. Rawat, and G. P. Joshi, "Naturally occurring xanthenes: chemistry and biology," *Journal of Applied Chemistry*, vol. 2013, Article ID 621459, 9 pages, 2013.
- [9] M. S. J. Nascimento, M. E. Sousa, and M. M. M. Pinto, "Xanthone derivatives: new insights in biological activities," *Current Medicinal Chemistry*, vol. 12, no. 21, pp. 2517–2538, 2005.
- [10] S. Martens and A. Mithöfer, "Flavones and flavone synthases," *Phytochemistry*, vol. 66, no. 20, pp. 2399–2407, 2005.
- [11] M. Singh, M. Kaur, and O. Silakari, "Flavones: an important scaffold for medicinal chemistry," *European Journal of Medicinal Chemistry*, vol. 84, pp. 206–239, 2014.
- [12] B. Jia, S. Li, X. Hu, G. Zhu, and W. Chen, "Recent research on bioactive xanthenes from natural medicine: *Garcinia hanburyi*," *AAPS PharmSciTech*, vol. 16, no. 4, pp. 742–758, 2015.
- [13] C. V. Simoben, A. Ibezim, F. Ntie-Kang, J. N. Nwodo, and L. L. Lifongo, "Exploring cancer therapeutics with natural products from African medicinal plants, part I: xanthenes, quinones, steroids, coumarins, phenolics and other classes of compounds," *Anti-Cancer Agents in Medicinal Chemistry*, vol. 15, no. 9, pp. 1092–1111, 2015.
- [14] A. K. Verma and R. Pratap, "The biological potential of flavones," *Natural Product Reports*, vol. 27, no. 11, pp. 1571–1593, 2010.
- [15] H. R. El-Seedi, M. A. El-Barbary, D. M. H. El-Ghorab et al., "Recent insights into the biosynthesis and biological activities of natural xanthenes," *Current Medicinal Chemistry*, vol. 17, no. 9, pp. 854–901, 2010.
- [16] D. Kingston, G. Cragg, and D. Newman, *Anticancer Agents from Natural Products*, CRC Press, 2005.
- [17] J. Qin, W. Lan, Z. Liu, J. Huang, H. Tang, and H. Wang, "Synthesis and biological evaluation of 1, 3-dihydroxyxanthone mannich base derivatives as anticholinesterase agents," *Chemistry Central Journal*, vol. 7, no. 1, article 78, 2013.
- [18] K. S. Bhullar and H. P. V. Rupasinghe, "Polyphenols: multipotent therapeutic agents in neurodegenerative diseases," *Oxidative Medicine and Cellular Longevity*, vol. 2013, Article ID 891748, 18 pages, 2013.
- [19] S. S. Panda, M. Chand, R. Sakhuja, and S. C. Jain, "Xanthenes as potential antioxidants," *Current Medicinal Chemistry*, vol. 20, no. 36, pp. 4481–4507, 2013.
- [20] H.-Y. Zhang, D.-P. Yang, and G.-Y. Tang, "Multipotent antioxidants: from screening to design," *Drug Discovery Today*, vol. 11, no. 15-16, pp. 749–754, 2006.
- [21] H.-F. Ji and H.-Y. Zhang, "Theoretical evaluation of flavonoids as multipotent agents to combat Alzheimer's disease," *Journal of Molecular Structure: THEOCHEM*, vol. 767, no. 1-3, pp. 3–9, 2006.
- [22] M. I. Cruz, *Xanthone and flavone derivatives as potential dual agents for Alzheimer's disease [M.S. thesis]*, Universidade do Porto, Porto, Portugal, 2015, <https://repositorio-aberto.up.pt/bitstream/10216/85633/2/36426.pdf>.
- [23] M.-H. Lee, R.-D. Lin, L.-Y. Shen, L.-L. Yang, K.-Y. Yen, and W.-C. Hou, "Monoamine oxidase B and free radical scavenging activities of natural flavonoids in *Melastoma candidum* D. Don," *Journal of Agricultural and Food Chemistry*, vol. 49, no. 11, pp. 5551–5555, 2001.
- [24] C. Brühlmann, A. Marston, K. Hostettmann, P.-A. Carrupt, and B. Testa, "Screening of non-alkaloidal natural compounds as acetylcholinesterase inhibitors," *Chemistry and Biodiversity*, vol. 1, no. 6, pp. 819–829, 2004.
- [25] A. Urbain, A. Marston, E. F. Queiroz, K. Ndjoko, and K. Hostettmann, "Xanthenes from *Gentiana campestris* as new acetylcholinesterase inhibitors," *Planta Medica*, vol. 70, no. 10, pp. 1011–1014, 2004.
- [26] F. Chimenti, R. Fioravanti, A. Bolasco et al., "A new series of flavones, thioflavones, and flavanones as selective monoamine oxidase-B inhibitors," *Bioorganic and Medicinal Chemistry*, vol. 18, no. 3, pp. 1273–1279, 2010.
- [27] I. Uriarte-Pueyo and M. I. Calvo, "Flavonoids as acetylcholinesterase inhibitors," *Current Medicinal Chemistry*, vol. 18, no. 34, pp. 5289–5302, 2011.
- [28] S. Rizzo, A. Cavalli, L. Ceccarini et al., "Structure-activity relationships and binding mode in the human acetylcholinesterase active site of Pseudo-irreversible inhibitors related to xanthostigmine," *ChemMedChem*, vol. 4, no. 4, pp. 670–679, 2009.
- [29] Y. Wang, Z. Xia, J.-R. Xu et al., " α -Mangostin, a polyphenolic xanthone derivative from mangosteen, attenuates β -amyloid oligomers-induced neurotoxicity by inhibiting amyloid aggregation," *Neuropharmacology*, vol. 62, no. 2, pp. 871–881, 2012.
- [30] R. C. Y. Choi, J. T. T. Zhu, A. W. Y. Yung et al., "Synergistic action of flavonoids, baicalein, and daidzein in estrogenic and neuroprotective effects: a development of potential health products and therapeutic drugs against Alzheimer's disease," *Evidence-Based Complementary and Alternative Medicine*, vol. 2013, Article ID 635694, 10 pages, 2013.
- [31] K. Jiménez-Aliaga, P. Bermejo-Bescós, J. Benedí, and S. Martín-Aragón, "Quercetin and rutin exhibit antiamyloidogenic and

- fibril-disaggregating effects in vitro and potent antioxidant activity in APPsw cells," *Life Sciences*, vol. 89, no. 25-26, pp. 939-945, 2011.
- [32] C. Uvarani, K. Chandraprakash, M. Sankaran, A. Ata, and P. S. Mohan, "Antioxidant and structure-activity relationships of five tetraoxygenated xanthenes from *Swertia minor* (Griseb.) Kobl," *Natural Product Research*, vol. 26, no. 13, pp. 1265-1270, 2012.
- [33] M. Grazul and E. Budzisz, "Biological activity of metal ions complexes of chromones, coumarins and flavones," *Coordination Chemistry Reviews*, vol. 253, no. 21-22, pp. 2588-2598, 2009.
- [34] Y. Hanasaki, S. Ogawa, and S. Fukui, "The correlation between active oxygens scavenging and antioxidative effects of flavonoids," *Free Radical Biology and Medicine*, vol. 16, no. 6, pp. 845-850, 1994.
- [35] L. Magnani, E. M. Gaydou, and J. C. Hubaud, "Spectrophotometric measurement of antioxidant properties of flavones and flavonols against superoxide anion," *Analytica Chimica Acta*, vol. 411, no. 1-2, pp. 209-216, 2000.
- [36] C. M. M. Santos, M. Freitas, D. Ribeiro et al., "2,3-Diaryl-xanthenes as strong scavengers of reactive oxygen and nitrogen species: a structure-activity relationship study," *Bioorganic and Medicinal Chemistry*, vol. 18, no. 18, pp. 6776-6784, 2010.
- [37] H. Cidade, V. Rocha, A. Palmeira et al., "In silico and in vitro antioxidant and cytotoxicity evaluation of oxygenated xanthone derivatives," *Arabian Journal of Chemistry*, 2017.
- [38] E. Costa, E. Sousa, N. Nazareth, M. S. J. Nascimento, and M. M. M. Pinto, "Synthesis of xanthenes and benzophenones as inhibitors of tumor cell growth," *Letters in Drug Design & Discovery*, vol. 7, no. 7, pp. 487-493, 2010.
- [39] E. Fernandes, A. M. S. Silva, J. A. S. Cavaleiro, F. M. Silva, M. F. M. Borges, and M. M. M. Pinto, "1H and Spectroscopy of Mono-, Di-, Tri- 13C NMR and Tetrasubstituted Xanthenes," *Magnetic Resonance in Chemistry*, vol. 36, pp. 305-309, 1998.
- [40] L. R. Fukumoto and G. Mazza, "Assessing antioxidant and prooxidant activities of phenolic compounds," *Journal of Agricultural and Food Chemistry*, vol. 48, no. 8, pp. 3597-3604, 2000.
- [41] W. Brand-Williams, M. E. Cuvelier, and C. Berset, "Use of a free radical method to evaluate antioxidant activity," *LWT—Food Science and Technology*, vol. 28, no. 1, pp. 25-30, 1995.
- [42] A. P. Vale, H. Cidade, M. Pinto, and M. B. P. P. Oliveira, "Effect of sprouting and light cycle on antioxidant activity of *Brassica oleracea* varieties," *Food Chemistry*, vol. 165, pp. 379-387, 2014.
- [43] T. C. P. Dinis, V. M. C. Madeira, and L. M. Almeida, "Action of phenolic derivatives (acetaminophen, salicylate, and 5-aminosalicylate) as inhibitors of membrane lipid peroxidation and as peroxyl radical scavengers," *Archives of Biochemistry and Biophysics*, vol. 315, no. 1, pp. 161-169, 1994.
- [44] J. E. Brown, H. Khodr, R. C. Hider, and C. A. Rice-Evans, "Structural dependence of flavonoid interactions with Cu²⁺ ions: implications for their antioxidant properties," *Biochemical Journal*, vol. 330, no. 3, pp. 1173-1178, 1998.
- [45] M. C. da Silva, H. Cidade, E. Sousa, and M. Pinto, "Searching for small molecules with antioxidant and anticoagulant properties to fight thrombosis," *American Journal of Pharmaceutical Sciences and Nanotechnology*, vol. 1, no. 1, pp. 43-50, 2014.
- [46] G. L. Ellman, K. D. Courtney, V. Andres Jr., and R. M. Featherstone, "A new and rapid colorimetric determination of acetylcholinesterase activity," *Biochemical Pharmacology*, vol. 7, no. 2, pp. 88-95, 1961.
- [47] J. Cheung, M. J. Rudolph, F. Burshteyn et al., "Structures of human acetylcholinesterase in complex with pharmacologically important ligands," *Journal of Medicinal Chemistry*, vol. 55, no. 22, pp. 10282-10286, 2012.
- [48] J. L. Sussman, D. Lin, J. Jiang et al., "Protein Data Bank (PDB): database of three-dimensional structural information of biological macromolecules," *Acta Crystallographica Section D: Biological Crystallography*, vol. 54, no. 6, part 1, pp. 1078-1084, 1998.
- [49] M. Froimowitz, "HyperChem: a software package for computational chemistry and molecular modeling," *BioTechniques*, vol. 14, no. 6, pp. 1010-1013, 1993.
- [50] O. Trott and A. J. Olson, "Software news and update AutoDock Vina: improving the speed and accuracy of docking with a new scoring function, efficient optimization, and multithreading," *Journal of Computational Chemistry*, vol. 31, no. 2, pp. 455-461, 2010.
- [51] D. Seeliger and B. L. de Groot, "Ligand docking and binding site analysis with PyMOL and Autodock/Vina," *Journal of Computer-Aided Molecular Design*, vol. 24, no. 5, pp. 417-422, 2010.
- [52] S. Vilar, G. Cozza, and S. Moro, "Medicinal chemistry and the Molecular Operating Environment (MOE): application of QSAR and molecular docking to drug discovery," *Current Topics in Medicinal Chemistry*, vol. 8, no. 18, pp. 1555-1572, 2008.
- [53] P. E. Eaton, G. R. Carlson, and J. T. Lee, "Phosphorus pentoxide-methanesulfonic acid. Convenient alternative to polyphosphoric acid," *Journal of Organic Chemistry*, vol. 38, no. 23, pp. 4071-4073, 1973.
- [54] N. Fonteneau, P. Martin, M. Mondon, H. Ficheux, and J.-P. Gesson, "Synthesis of quinone and xanthone analogs of rhein," *Tetrahedron*, vol. 57, no. 44, pp. 9131-9135, 2001.
- [55] S. v. Kostanecki and B. Nessler, "Synthesen von Oxyxanthenen," *Berichte der deutschen chemischen Gesellschaft*, vol. 24, no. 1, pp. 1894-1897, 1891.
- [56] C. M. G. Azevedo, C. M. M. Afonso, and M. M. M. Pinto, "Routes to xanthenes: an update on the synthetic approaches," *Current Organic Chemistry*, vol. 16, no. 23, pp. 2818-2867, 2012.
- [57] S. Zhang, J. Ma, Y. Bao et al., "Nitrogen-containing flavonoid analogues as CDK1/cyclin B inhibitors: synthesis, SAR analysis, and biological activity," *Bioorganic and Medicinal Chemistry*, vol. 16, no. 15, pp. 7127-7132, 2008.
- [58] S. Altamura and M. U. Muckenthaler, "Iron toxicity in diseases of aging: Alzheimer's disease, Parkinson's disease and atherosclerosis," *Journal of Alzheimer's Disease*, vol. 16, no. 4, pp. 879-895, 2009.
- [59] V. Chauhan and A. Chauhan, "Oxidative stress in Alzheimer's disease," *Pathophysiology*, vol. 13, no. 3, pp. 195-208, 2006.
- [60] A. Gella and N. Durany, "Oxidative stress in Alzheimer disease," *Cell Adhesion and Migration*, vol. 3, no. 1, pp. 88-93, 2009.
- [61] M. B. Colovic, D. Z. Krstic, T. D. Lazarevic-Pasti, A. M. Bondzic, and V. M. Vasic, "Acetylcholinesterase inhibitors: pharmacology and toxicology," *Current Neuropharmacology*, vol. 11, no. 3, pp. 315-335, 2013.
- [62] S.-H. Lu, J. W. Wu, H.-L. Liu et al., "The discovery of potential acetylcholinesterase inhibitors: a combination of pharmacophore modeling, virtual screening, and molecular docking studies," *Journal of Biomedical Science*, vol. 18, no. 1, article 8, 2011.

- [63] H. Dvir, I. Silman, M. Harel, T. L. Rosenberry, and J. L. Sussman, "Acetylcholinesterase: from 3D structure to function," *Chemico-Biological Interactions*, vol. 187, no. 1–3, pp. 10–22, 2010.
- [64] J. Barbosa, R. T. Lima, D. Sousa et al., "Screening a small library of xanthenes for antitumor activity and identification of a hit compound which induces apoptosis," *Molecules*, vol. 21, no. 1, p. 81, 2016.



Hindawi

Submit your manuscripts at
<https://www.hindawi.com>

